J. Biochem. 131, 407–418 (2002)

Ca^{2+}- and S1-Induced Conformational Changes of Reconstituted Skeletal Muscle Thin Filaments Observed by Fluorescence Energy Transfer Spectroscopy: Structural Evidence for Three States of Thin Filament[1]

Hong Hai,* Ken-Ichi Sano,† Kayo Maeda,† Yuichiro Maéda,† and Masao Miki*,[2]

**Department of Applied Chemistry and Biotechnology, Fukui University, 3-9-1 Bunkyo, Fukui 910-8507, and †Riken Harima Institute at Spring8, Mikazuki-cho, Sayo, Hyogo, 679-5143*

Received November 28, 2001; accepted December 22, 2001

Rabbit skeletal muscle α-tropomyosin (Tm) and the deletion mutant (D234Tm) in which internal actin-binding pseudo-repeats 2, 3, and 4 are missing [Landis *et al.* (1997) *J. Biol. Chem.* 272, 14051–14056] were used to investigate the interaction between actin and tropomyosin or actin and troponin (Tn) by means of fluorescence resonance energy transfer (FRET). FRET between Cys-190 of D234Tm and Gln-41 or Cys-374 of actin did not cause any significant Ca^{2+}-induced movement of D234Tm, as reported previously for native Tm [Miki *et al.* (1998) *J. Biochem.* 123, 1104–1111]. FRET did not show any significant S1-induced movement of Tm and D234Tm on thin filaments either. The distances between Cys-133 of TnI, and Gln-41 and Cys-374 of actin on thin filaments reconstituted with D234Tm (mutant thin filaments) were almost the same as those on thin filaments with native Tm (wild-type thin filaments) in the absence of Ca^{2+}. Upon binding of Ca^{2+} to TnC, these distances on mutant thin filaments increased by ~10 Å in the same way as on wild-type thin filaments, which corresponds to a Ca^{2+}-induced conformational change of thin filaments [Miki *et al.* (1998) *J. Biochem.* 123, 324–331]. The rigor binding of myosin subfragment 1 (S1) further increased these distances by ~7 Å on both wild-type and mutant thin filaments when the thin filaments were fully decorated with S1. This indicates that a further conformational change on thin filaments was induced by S1 rigor-binding (S1-induced or open state). Plots of the extent of S1-induced conformational change *vs.* molar ratio of S1 to actin showed that the curve for wild-type thin filaments is hyperbolic, whereas that for mutant thin filaments is sigmoidal. This suggests that the transition to the S1-induced state on mutant thin filaments is depressed with a low population of rigor S1. In the absence of Ca^{2+}, the distance also increased on both wild-type and mutant thin filaments close to the level in the presence of Ca^{2+} as the molar ratio of S1 to actin increased up to 1. The curves are sigmoidal for both wild-type and mutant thin filaments. The addition of ATP completely reversed the changes in FRET induced by rigor S1 binding. For mutant thin filaments, the transition from the closed state to the open state in the presence of ATP is strongly depressed, which results in the inhibition of acto-myosin ATPase even in the presence of Ca^{2+}. The present FRET measurements provide structural evidence for three states of thin filaments (relaxed, Ca^{2+}-induced or closed, and S1-induced or open states) for the regulation mechanism of skeletal muscle contraction.

Key words: FRET, regulation, thin filament, three states of thin filament, troponin.

Striated muscle contraction is initiated by the binding of Ca^{2+} to troponin (Tn) (*1*). Tn consists of three different subunits (TnI, TnT, and TnC) and is located periodically along a thin filament with tropomyosin (Tm). Numerous studies have characterized the interaction between the thin filament proteins to deduce how the Ca^{2+}-triggering signal is propagated from TnC to the rest of a thin filament [for a review, see Gordon *et al.*, (*2*)]. Structural studies, such as 3D-image reconstructions of electron micrographs (3D-EM) and X-ray diffraction, on regulation of the actin-myosin

[1] This study was performed through the Special Coordination Funds of the Ministry of Education, Culture, Sports, Science and Technology, the Japanese Government.

[2] To whom correspondence should be addressed. Tel: +81-776-27-8786, Fax: +81-776-27-8747, E-mail: masao@acbio.fukui-u.ac.jp

Abbreviations: 3D-EM, three-dimensional image reconstruction of electron micrographs; DABMI, 4-dimethyl-aminophenylazophenyl 4′-maleimide; DTT, dithiothreitol; EGTA, ethylene glycol-bis (2-aminoethyl ether)-*N,N,N′,N′*-tetraacetic acid; FLC, fluorescein cadaverine; FRET, fluorescence resonance energy transfer; IAEDANS, 5-(2-iodoacetylaminoethyl)aminonaphthalene 1-sulfonic acid; S1, myosin subfragment 1; Tm, tropomyosin; D234eTm, rabbit Ala-Ser-α-tropomyosinΔ(49-167), which was expressed by *Escherichia coli*; D234bTm, rabbit α-tropomyosinΔ(49-167), which was expressed by the Sf9-baculovirus system; Tn, troponin.

interaction in vertebrate striated thin filaments led to the steric blocking model [(*3*) and for a review, see Amos (*4*)]. In this model, Tm is located along the actin filament at a position where it can influence the actin–myosin interaction, and upon activation Tm moves from a position where it blocks the actin-myosin interaction to one where it allows it. The results of X-ray diffraction studies, measuring changes in the intensity of the second layer line upon activation in whole muscle, were interpreted as showing the movement of Tm at the periphery of a thin filament to a position in the groove of the actin long helix. More recent biochemical studies have suggested that there may be three states of thin filaments (blocked, closed, and open) (*5–7*). The equilibrium between the blocked and closed states is Ca^{2+}-sensitive and strong S1 binding induces the fully activated open state. Recent X-ray diffraction studies of skinned fibers and oriented filaments, and 3D-EM studies of isolated thin filaments have shown three positions of Tm corresponding to the three state model (*8, 9*). However, on interpretation of both X-ray and 3D-EM measurements the presence of Tn, and possible changes in Tn and the actin structure with Ca^{2+} are not taken into consideration. Furthermore, for electron microscope observation, thin filaments are fixed, hydrated and stained, which might distort the molecular arrangements of the thin filaments. Therefore, it is still not clear whether the conformational change observed on both X-ray and 3D-EM measurements could be entirely attributed to movement of Tm or to changes in the Tn position and/or in actin structure (*10*).

Fluorescence resonance energy transfer (FRET) has been extensively used for studying the spatial relationships between residues on muscle proteins (*11, 12*). This method is especially valuable for detecting a small conformational change, since the transfer efficiency is a function of the inverse of the sixth power of the distance between probes. For this method, fluorescence donor and acceptor molecules are specifically labeled so that the assignment of the conformational change is direct. Furthermore, this method reveals the dynamic structures of a protein assembly in solution and can detect a very rapid conformational change, *i.e.* on a milliseconds time scale, in combination with a stopped flow apparatus (*13*). Several attempts have been made to detect the movement of Tm and Tn on a reconstituted thin filament in response to a change in the Ca^{2+} concentration. With Ca^{2+} binding to TnC, the distances between Cys-133 of TnI, and Cys-374, Gln-41 or the nucleotide binding site of actin increased by 10–15 Å (*14–16*). However, the efficiency of transfer between probes attached to Tm (at position 87 or 190) and actin (at position 41, 61, or 374, or the nucleotide-binding site) was not so sensitive to the Ca^{2+} ion concentration, as expected from the steric blocking model (*17–19*).

The Tm molecule contains seven quasiequivalent regions, each of which contains a pair of putative actin-binding motifs. Several deletion mutants of Tm have been constructed in order to understand the involvement of the specific regions in regulatory function (*20–24*). Deletion of one complete such repeat has little effect on the physiological function of Tm (*20*). Tropomyosins of four periods long can regulate the actomyosin ATPase in the absence of Ca^{2+}, but relief of inhibition in the presence of Ca^{2+} was severely impaired (*21–23*). Myosin S1-induced binding of Tm to actin was lost in all mutants lacking period 5 (166–207 amino acid residues) (*23*). D234Tm, in which three of seven such repeats (49–167 amino acid residues) have been deleted, retains the ability to bind normally to actin and Tn, but it inhibits actomyosin MgATPase and filament sliding *in vitro*, which is not reversed by Ca^{2+} and Tn (*21*). 3D-EM of thin filaments containing actin, Tn and Tm or D234Tm showed that in the presence and absence of Ca^{2+}, the D234Tm position was indistinguishable from that of Tm, suggesting that the mutation did not affect normal Tm movement induced by Ca^{2+} and Tn (*24*). In the present study, D234Tm, in comparison with native Tm, was used for FRET measurements in order to determine what conformational changes are critical for the regulation mechanism. Ca^{2+}-induced and S1-induced movements of Tm and D234Tm on a reconstituted thin filament were examined by FRET between Cys-190 of Tm or D234Tm and Gln-41 or Cys-374 of actin. However, no appreciable Ca^{2+}-induced or S1-induced movement of Tm and D234Tm on the reconstituted thin filaments was observed in contrast to a report of 3D-EM analysis (*24*). Furthermore, we measured the FRET between Cys-133 of TnI and Gln-41 or Cys-374 of actin on a reconstituted thin filament containing Tm or D234Tm comparatively. The effect of S1 on the reconstituted thin filaments was also measured under these conditions by FRET. The present FRET measurements demonstrated that an S1-induced conformational change on thin filaments is critical for active interaction of actomyosin during the ATP cycle.

MATERIALS AND METHODS

Reagents—Phallodin from *Amantina phalloides* was purchased from Boehringer Mannheim Biochemica. IAEDANS, DABMI, and FLC were purchased from Molecular Probes. BCA Protein assay reagent was from Pierce Chemicals. All other chemicals were of analytical grade.

Protein Preparation—Actin was prepared from acetone-dried powder of rabbit skeletal muscle according to the method of Spudich and Watt (*25*). S1 was prepared from rabbit skeletal muscle myosin by chymotryptic digestion according to the method of Weeds and Pope (*26*). Tn was extracted from the rabbit skeletal muscle after extraction of myosin, and purified by the method of Ebashi *et al.* (*27*). α-Tm was extracted from rabbit hearts as previously reported (*19*). Microbial transglutaminase was a generous gift from the Food Research and Development Laboratories, Ajinomoto. In contrast to transglutaminase from guinea pigs, this enzyme does not require Ca^{2+} ions for its activity (*28, 29*).

Expression and transfer vectors of D234Tm were constructed as follows. Firstly, rabbit skeletal muscle α-Tm cDNA in M13mp18 (*30*) was mutagenized by single-stranded site-directed mutagenesis (Amersham, Sculptor *in vitro* mutagenesis system) to mutate +22 T to G to introduce a *Pst*I site. Secondly, the *Pst*I and *Bam*HI fragment of Tm was ligated to both the annealed oligonucleotides, which contained the N-terminal sequence of Tm with an additional MAS sequence and pTV118N, which was digested by *Nco*I and *Bam*HI. Thirdly, PCR was carried out to generate a circular plasmid lacking a region that encodes 49–167 amino acid residues. This plasmid was named pTV-R-MAS-TmD (49–167). Then, the *Nco*I and *Bam*HI fragment of pTV-R-MAS-TmD (49–167) was inserted into the

*Nco*I and *Bam*HI sites of pET3d to obtain the expression vector of bacterial expression, pET-R-MAS-TmD (49–167). On the other hand, the transfer vector for expression using the Sf9-baculovirus system, pVL-TmD (49–167), was generated as follows. PCR was carried out to remove the additional MAS from pTV-R-MAS-TmD (49–167), followed by ligation into the *Xba*I–*Bam*HI site of pVL1392 with extra-leader sequences (described elsewhere). Transfection and expression of TmD (49–167) were performed according to Miegel *et al.* (*31*). The oligonucleotide sequence for mutagenesis of +22 T to G was 5′-CGTAGACGTCGAAGAAGAA-3′. The annealed oligonucleotides which contain the N-terminal sequence of Tm with MAS were 5′-CATGGCGAG-CATGGATGCGATCAAGAAGAAGATGCA-3′ and 5′-TCTT-CTTCTTGATCGCATCCATGCTCGC-3′. The oligonucleotides for PCR to delete 49–167 were 5′-CTTTTGTAGCGA-CACCAGCTCATCTTCC-3′ and 5′-AAGCTGGTCATCATT-GAGAGCGACCTGGAGCG-3′. The oligonucleotides for PCR to remove MAS and cloning into pVL1392 with extra-leader sequences were 5′-CCATGGACGCCATCAAGAAG-AAGATGCAGATGCTGAAGC-3′ and 5′-CTCGGGATCCG-TGAGACAAAGAAAC-3′. The expression in *Escherichia coli* (D234eTm) or the Sf9-baculovirus system (D234bTm), and purification of mutant Tm were carried out according to Kluwe *et al.* (*30*), and Miegel *et al.* (*31*).

Protein concentrations were determined by use of absorption coefficients of $A_{290\,nm}$ = 0.63 $(mg/ml)^{-1}$ cm^{-1} for G-actin, $A_{280\,nm}$ = 0.75 $(mg/ml)^{-1}$ cm^{-1} for S1, 0.33 $(mg/ml)^{-1}$ cm^{-1} for Tm, 0.45 $(mg/ml)^{-1}$ cm^{-1} for Tn, and 1.024×10^4 M^{-1} cm^{-1} for D234Tm (*21*). The concentrations of labeled proteins were measured with the BCA protein assay reagent with the respective unlabeled proteins as standards. Relative molecular masses of 43,000 for actin, 115,000 for S1, 66,000 for Tm, 37,700 for D234Tm, 69,000 for Tn, and 38,000 for transglutaminase were used.

Labeling of Proteins—Labeling of actin at Gln-41 with fluorescein cadaverin (FLC) was carried out according to the method of Takashi (*32*). Microbial transglutaminase was used instead of that from guinea pig. G-actin (50 μM) was incubated for 20 h at 4°C with a fivefold molar excess of FLC in 5 mM Tris-HCl (pH 8.0), 0.5 mM ATP, 1 mM DTT, 1 mM NaN_3, and 1.5 μM transglutaminase. The labeled actin was polymerized in 50 mM NaCl and 2 mM $MgCl_2$, and then centrifuged at 40,000 rpm for 90 min. The pellet was suspended in 0.1 M NaCl, 2 mM $MgCl_2$, and 0.5 mM DTT, and then centrifuged again to remove unreacted FLC. The labeled actin pellet was suspended in 2 mM Tris-HCl (pH 8.0), 0.1 mM ATP, 0.1 mM $CaCl_2$, and 0.25 mM DTT, and then dialyzed against the same buffer solution. The amount of FLC bound to actin was determined by using the extinction coefficient of 75,500 M^{-1} cm^{-1} at 493 nm (*33*). Labeling of actin at Cys-374 with DABMI was carried out as previously reported (*16*). G-actin (50 μM) was incubated for 6 h at 4°C with a fivefold molar excess of DABMI in 0.5 mM ATP, 0.1 mM $CaCl_2$, and 2 mM Tris-HCl (pH 8.0). The reaction was stopped by the addition of 1 mM DTT. The sample was centrifuged at 30,000 rpm for 15 min to remove unreacted DABMI. The supernatant was polymerized in 0.1 M KCl and 2 mM $MgCl_2$, and then centrifuged at 40,000 rpm for 90 min. The pellet was suspended in 1 mM ATP, 0.1 mM $CaCl_2$, and 2 mM Tris-HCl (pH 8.0), following dialysis against 0.1 mM ATP, 0.1 mM $CaCl_2$, and 2 mM Tris-HCl (pH 8.0). The sample solution was clarified by centrifugation at 100,000 rpm for 10 min. The ratio labeling of DABMI to actin was measured by use of the absorption coefficient of 24,800 M^{-1} cm^{-1} at 460 nm (*34*).

Labeling of Cys-133 of TnI with IAEDANS was carried out as previously reported (*16*). Tn was mixed with a fivefold molar excess of IAEDANS in 30 mM KCl, 10 mM phosphate buffer (pH 7.0), 1 mM $MgCl_2$, and 1 mM EGTA. After 4 h, the reaction was terminated by the addition of 10 mM DTT. The labeled Tn was fractionated between 40 and 60% ammonium sulfate saturation at 10,000 rpm for 20 min. The pellet was dissolved in 2 mM Tris-HCl (pH 8.0) and 1 mM 2-mercaptoethanol, and then dialyzed against the same buffer solution.

For labeling of Cys-190 of Tm and D234Tm with IAEDANS, 20 mg Tm (or D234Tm) was incubated at 37°C for 2 h in 20 mM Tris-HCl (pH 8.0) and 10 mM DTT. The pH of the sample was adjusted to 4.5 with 0.1 N HCl, followed by centrifugation at 12,000 rpm for 10 min. The pellet was suspended in 40 mM phosphate buffer (pH 7.0), 1 M KCl, and 1 mM EDTA. The sample solution was mixed with a ten-fold molar excess of IAEDANS at 37°C for 24 h. The reaction was terminated by the addition of 1 mM DTT and the labeled Tm was fractionated by 70% ammonium sulfate saturation at 12,000 rpm for 20 min. The pellet was resuspended in 2 mM Tris-HCl (pH 8.0) and 1 mM DTT, following exhaustive dialysis against the same solution. The IAEDANS to Tm (or D234Tm) labeling ratio was measured by use of the absorption coefficient of 6100 M^{-1} cm^{-1} at 337 nm (*35*). Figure 1 is a schematic representation of the Tn-Tm complex with labeling sites on TnI, Tm and D234Tm.

Spectroscopic Measurements—Absorption was measured with a Hitachi U2000 spectrophotometer. Steady-state fluorescence was measured with a Perkin Elmer LS50B fluorometer. Light scattering was measured at 550 nm at a 90° angle, using the fluorometer. The temperature was main-

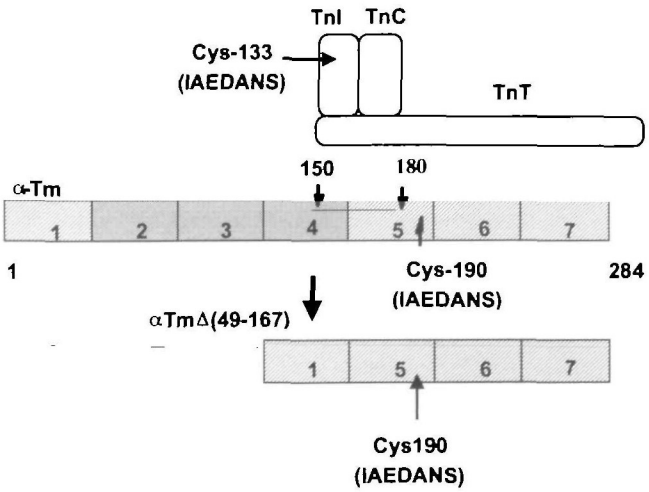

Fig. 1. **A schematic representation of the troponin-tropomyosin complex with the donor-labeling sites on Cys-133 of TnI, and Cys-190 of Tm and D234Tm.** The Tm molecule contains seven quasiequivalent region, each of which contains a pair of putative actin-binding motifs. In D234Tm, three of seven such repeats (amino acid residues 49–167) are deleted. X-ray analysis of co-crystals of tropomyosin and troponin revealed that the head region of the troponin complex binds tropomyosin near residues 150–180 (*59*).

tained at 20°C.

Fluorescence Resonance Energy Transfer—The efficiency, E, of resonance energy transfer between probes was determined by measuring the fluorescence intensity of the donor in both the presence (F_{DA}) and absence (F_{DO}) of the acceptor, as given by

$$E = 1-F_{DA}/F_{DO} \quad (1)$$

The efficiency is related to the distance (R) between the donor and acceptor, and Förster's critical distance (R_0) at which the transfer efficiency is equal to 50%

$$E = R^6/(R^6 + R_0^6) \quad (2)$$

R_0 can be obtained (in nm) with

$$R_0 = (8.79 \times 10^{-11})\, n^{-4}\, \kappa^2\, Q_0 J \quad (3)$$

where n is the refractive index of the medium taken as 1.4, κ^2 is the orientation factor, Q_0 is the quantum yield of the donor in the absence of the acceptor, and J is the spectral overlap integral between the donor emission $F_D(\lambda)$ and acceptor absorption $\varepsilon_A(\lambda)$ spectra defined by

$$J = \int F_D(\lambda)\, \varepsilon_A(\lambda)\, \lambda^4\, d\lambda / \int F_D(\lambda)\, d\lambda \quad (4)$$

The quantum yield was determined by means of a comparative method using quinine sulfate in 1 M H_2SO_4 as the standard, which has an absolute quantum yield of 0.70 (*36*). κ^2 was taken as 2/3 for the calculation of distances. The decrease in the fluorescence intensity due to inner filter effects was corrected with

$$F_c = F_{obs} \times 10^{(A_{ex}+A_{em})/2} \quad (5)$$

Where A_{ex} and A_{em} are the absorption of the sample at the excitation and emission wavelengths, respectively.

Other Methods—MgATPase activity was measured by the method of Tausky and Shorr (*37*). Measurements were performed at 25°C in 10 mM KCl, 5 mM $MgCl_2$, 2 mM ATP, 20 mM Tris-HCl (pH 8.0), 1 mM DTT, and 50 μM $CaCl_2$ for the $+Ca^{2+}$ state or 1 mM EGTA for the $-Ca^{2+}$ state. The protein concentrations were: 4 μM F-actin, 1 μM S1, 0, 0.2, 0.4, 0.6, 0.8, and 1.0 μM Tm (or D234Tm), and 0, 0.3, 0.5, 0.7, 0.9, and 1.1 μM Tn.

RESULTS

The MgATPase activity of the reconstituted system composed of F-actin, S1, Tn, and Tm or D234eTm was measured in the presence and absence of Ca^{2+} ions. The D234eTm and Tn complex inhibited actoS1-MgATPase activity in the absence of Ca^{2+} ions as efficiently as the Tm and Tn complex, but this inhibition was not released by the addition of Ca^{2+} ions, as reported by Landis *et al.* (*21*).

The AEDANS moiety bound to Cys-133 of TnI or Cys-190 of Tm and D234eTm was used as the energy transfer donor, while FLC or DABMI attached to Gln-41 or Cys-374 of actin, respectively, was used as the energy transfer acceptor. Several attempts have been made to detect a difference in the conformational change between thin filaments reconstituted with Tm (wild-type thin filaments) and D234eTm (mutant thin filaments), to understand why D234eTm always inhibits the actoS1-MgATPase activity whether Ca^{2+} is present or not.

FRET between Cys-133 of TnI and Gln-41 or Cys-374 of Actin on Thin Filaments Reconstituted with Tm or D234eTm—The overlap integral, J, was calculated to be 18.7×10^{14} M^{-1} cm^{-1} nm^4 for the AEDANS-Tn/FLC-F-actin pair and 6.42×10^{14} M^{-1} cm^{-1} nm^4 for the AEDANS-Tn/DABMI-F-actin pair. By taking n = 1.4, κ^2 = 2/3, and Q_0 = 0.31, the Förster's critical distance, R_0, was determined to be 45.5 Å for the AEDANS-Tn/FLC-F-actin pair and 38.1 Å for the AEDANS-Tn/DABMI-F-actin pair.

Figure 2 shows the fluorescence spectra of AEDANS-Tn on the mutant thin filaments in the presence (curves 2 and 5) and absence (curves 1 and 4) of an acceptor (FLC-actin). The solvent conditions were 30 mM KCl, 20 mM Tris-HCl (pH 7.6), 2 mM $MgCl_2$, 0.1 mM ATP, 1 mM NaN_3 (buffer F), and 50 μM $CaCl_2$ ($+Ca^{2+}$ state) or 1 mM EGTA ($-Ca^{2+}$ state) at 20°C. The donor fluorescence was significantly quenched in the presence of the acceptor at wavelengths shorter than 480 nm on the mutant thin filaments. This can be attributed mainly to resonance energy transfer from AEDANS-Tn to FLC-actin. Removal of free Ca^{2+} ions by the addition of 1 mM EGTA increased the donor fluorescence intensity in the absence of the acceptor, but decreased it significantly in the presence of the acceptor. In the absence of Ca^{2+}, the extent of transfer efficiency was greater than that in the presence of Ca^{2+} on the mutant thin filaments. These spectra were exactly the same as those for wild-type thin filaments reported previously (*16*). This indicates that the distance between Gln-41 of actin and Cys-133 of TnI decreased upon the addition of EGTA regardless of whether the thin filaments were reconstituted with Tm or D234eTm.

In addition, a similar result was obtained in Fig. 3, which shows FRET between Cys-374 on actin and Cys-133 on TnI on the mutant thin filaments. Fluorescence spectra were measured under the same conditions but with DABMI

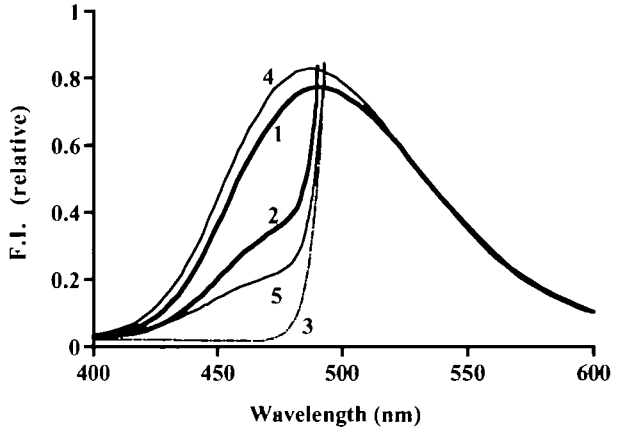

Fig. 2. **Fluorescence spectra of AEDANS bound to Cys-133 of TnI on reconstituted thin filaments with D234eTm in the presence and absence of an acceptor (FLC bound to Gln-41 of actin).** (1) F-actin/D234eTm/AEDANS-Tn/+Ca, (2) FLC-F-actin/D234eTm/AEDANS-Tn/+Ca, (3) FLC-F-actin/D234eTm/Tn/±Ca, (4) F-actin/D234eTm/AEDANS-Tn/–Ca, (5) FLC-F-actin/D234eTm/AEDANS-Tn/–Ca. Spectra were measured at 20°C in 30 mM KCl, 2 mM $MgCl_2$, 20 mM Tris-HCl (pH7.6), 0.1 mM ATP, 1 mM NaN_3 (buffer F), and 50 μM $CaCl_2$ for the $+Ca^{2+}$ state or 1 mM EGTA for the $-Ca^{2+}$ state. The concentrations of actin, Tm and Tn were 0.2, 0.044, and 0.046 mg/ml, respectively. Excitation was at 340 nm. The fluorescence spectra of curves 2, 3, and 5 at wavelengths longer than 480 nm, which are derived mainly from FLS with an emission peak at 520 nm, are omitted from the figure.

bound to Cys-374 as the acceptor instead of FLC bound to Gln-41 of actin.

To obtain more quantitative data for the transfer efficiency, the ratio of donor quenching was measured by titrating AEDANS-Tn/Tm or D234eTm with FLC-F-actin in the presence (buffer F + 50 μM $CaCl_2$) or absence of Ca^{2+} ions (buffer F + 1 mM EGTA) at 20°C (Fig. 4). The fluorescence intensity was measured at 460 nm, where no contribution of the acceptor-fluorescence from FLC occurs, as can be seen in Fig. 2. For correction of the fluorescence intensity change of AEDANS-Tn upon binding to an actin filament, the same amount of non-labeled F-actin was added to AEDANS-Tn/Tm or D234eTm as a reference, and the ratio of these fluorescence intensities was taken as the relative fluorescence intensity. The apparent decrease in the fluorescence intensity due to the inner filter effects arising from the absorbance of FLC-actin was corrected according to Eq. 5. The relative fluorescence intensity decreased gradually in the actin/Tn molar ratio range up to 7 and became almost constant in the range over 7 on the wild-type thin filaments, while on the mutant thin filaments the saturation point was 4. From the saturation points, the apparent energy transfer efficiencies given by Eq. 1 were 0.40 ± 0.02 for the $+Ca^{2+}$ state and 0.73 ± 0.02 for the $-Ca^{2+}$ state in the case of Tm, and 0.42 ± 0.02 for the $+Ca^{2+}$ state and 0.71 ± 0.02 for the $-Ca^{2+}$ state in the case of D234eTm. There was no significant difference in the extent of the transfer efficiency between the wild-type and mutant thin filaments. Taking into account a labeling ratio of FLC to actin of 0.91, the transfer efficiencies were calculated to be 0.44 ± 0.02 and 0.46 ± 0.02 for the $+Ca^{2+}$ state and 0.80 ± 0.02 and 0.78 ± 0.02 for the $-Ca^{2+}$ state in the case of Tm and D234eTm, respectively. These transfer efficiencies correspond to distances of 47.4 ± 0.7 Å and 46.7 ± 0.7 Å for the $+Ca^{2+}$ state and 36.1 ± 0.8 Å and 36.8 ± 0.7 Å for the $-Ca^{2+}$ state in the case of Tm and D234eTm, respectively.

AEDANS-Tn/Tm and AEDANS-Tn/D234eTm were also titrated with DABMI-F-actin in the same way as FLC-F-actin. The apparent energy transfer efficiencies were 0.42 ± 0.02 and 0.37 ± 0.02 for the $+Ca^{2+}$ state and 0.75 ± 0.02 and 0.71 ± 0.02 for the $-Ca^{2+}$ state in the case of Tm and D234eTm, respectively. The labeling ratio of DABMI to actin was 1.0. Then, these transfer efficiencies correspond to distances of 40.2 ± 0.6 and 41.6 ± 0.6 Å for the $+Ca^{2+}$ state and 31.7 ± 0.6 and 32.8 ± 0.5 Å for the $-Ca^{2+}$ state in the case of Tm, and D234eTm respectively. The results indicate that the mutation on Tm did not affect normal Ca^{2+}-induced movement of Tn on thin filaments. The transfer efficiencies and distances are summarized in Table I.

FRET between Cys-190 of Tm or D234Tm and Gln-41 or Cys-374 of Actin on Reconstituted Thin Filaments—Cys-190 of Tm or D234eTm was labeled with AEDANS to detect a distance change between Cys-190 of Tm and Gln-41or Cys-394 of actin. In the case of FLC-actin as the acceptor, the overlap integral, J, was calculated to be 14.3×10^{14} M^{-1} cm^{-1} nm^4 for both AEDANS-Tm and AEDANS-D234eTm. In the case of DABMI-actin as the acceptor, J was determined to be 5.85×10^{14} M^{-1} cm^{-1} nm^4 for both AEDANS-Tm and AEDANS-D234eTm. By taking n = 1.4, κ^2 = 2/3, and Q_0 = 0.29 for AEDANS-Tm or 0.28 for AEDANS-D234eTm, the

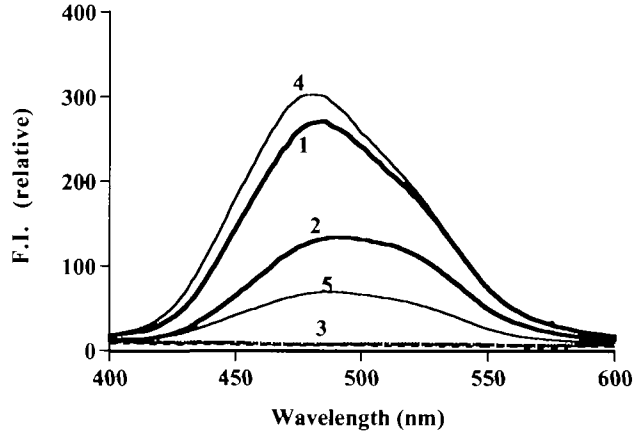

Fig. 3. **Fluorescence spectra of AEDANS bound to Cys-133 of TnI in reconstituted thin filaments with D234eTm in the presence and absence of an acceptor (DABMI bound to Cys-374 of actin).** (1) F-actin/D234eTm/AEDANS-Tn/+Ca, (2) DABMI-F-actin/D234eTm/AEDANS-Tn/+Ca, (3) DABMI-F-actin/D234eTm/Tn/±Ca, (4) F-actin/D234eTm/AEDANS-Tn/–Ca, (5) DABMI-F-actin/D234eTm/AEDANS-Tn/–Ca. Spectra were measured under the same conditions as in Fig. 2.

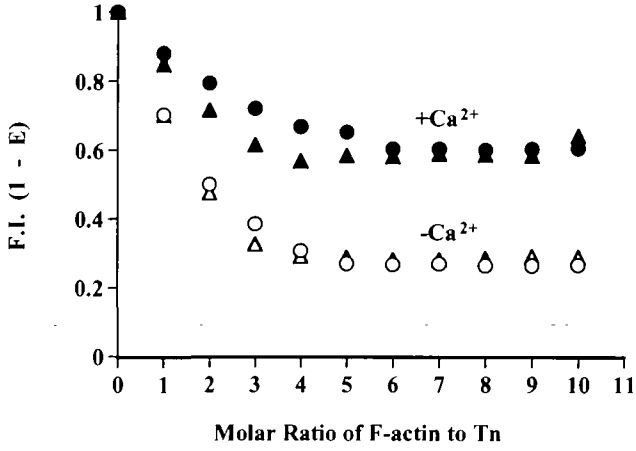

Fig. 4. **Relative fluorescence intensities of AEDANS bound to Cys-133 of TnI in reconstituted thin filaments with Tm (● for $+Ca^{2+}$ and ○ for $-Ca^{2+}$ state) or D234eTm (▲ for $+Ca^{2+}$ and △ for $-Ca^{2+}$ state) *vs.* molar ratio of FLC-F-actin to Tn.** Values were obtained in buffer F and 50 μM $CaCl_2$ for the $+Ca^{2+}$ state or 1 mM EGTA for the $-Ca^{2+}$ state at 20°C, after correction of the inner filter effects according to Eq. 5. The concentrations of Tm and Tn were 0.044 and 0.046 mg/ml, respectively. Excitation was at 340 nm and emission was measured at 460 nm.

TABLE I. **Distances between probes attached to Tn and actin in reconstituted thin filaments in the presence and absence of Ca^{2+} ions.**

Donor site (Cys133 of TnI)	Acceptor site (actin)	R_0(2/3) (Å)	Efficiency (+Ca/-Ca)	R(2/3) (Å) (+Ca/-Ca)
Tn/Tm	Gln-41	45.5	0.44 ± 0.02/ 0.80 ± 0.02	47.4 ± 0.7/ 36.1 ± 0.8
	Cys-374	38.1	0.42 ± 0.02/ 0.75 ± 0.02	40.2 ± 0.6/ 31.7 ± 0.6
Tn/D234eTm	Gln-41	45.5	0.46 ± 0.02/ 0.78 ± 0.02	46.7 ± 0.7/ 36.8 ± 0.7
	Cys-374	38.1	0.37 ± 0.02/ 0.71 ± 0.02	41.6 ± 0.6/ 32.8 ± 0.5
Tn/D234bTm	Cys-374	38.1	0.41 ± 0.03/ 0.71 ± 0.02	40.5 ± 0.8/ 32.8 ± 0.5

Förster's critical distance, R_0, was calculated to be 43.0 Å for AEDANS-Tm and 42.8 Å for AEDANS-D234eTm in the case of FLC-F-actin as the acceptor, and 37.1 Å for AEDANS-Tm and 36.8 Å for D234eTm in the case of DABMI-F-actin as the acceptor.

The fluorescence spectra of AEDANS bound to Tm or D234eTm on the reconstituted thin filaments in the presence and absence of an acceptor (FLC or DABMI bound to actin) were measured in buffer F + 50 μM $CaCl_2$ for the $+Ca^{2+}$ state or +1 mM EGTA for the $-Ca^{2+}$ state at 20°C. In the cases of both AEDANS-Tm and AEDANS-D234eTm, the donor fluorescence was significantly quenched in the presence of the acceptor (FLC- or DABMI-F-actin), but removal of free Ca^{2+} ions from Tn did not change the spectra in either the presence or absence of the acceptors. This suggests that the position of tropomyosin (at least a region including Cys-190) does not change during Ca^{2+}-induced conformational change of a thin filament. On the other hand, the extent of quenching in the case of AEDANS-D234eTm/FLC-F-actin was greater than in that of AEDANS-Tm/FLC-F-actin. The former extent was almost the same as that in the case of mutant α-Tm in which unique cysteine residue Cys-87 was labeled with IAEDANS, as previously reported (*19*). Both the mutant α-Tm (S-87-C, C-190-I) and D234eTm were expressed by *E. coli,* and have an extra dipeptide (Ala-Ser) at the N-terminus in order to restore actin binding and polymerization, and the N-terminus is not acetylated (*38*). Usually the p*K* value of the N-terminal amino group is low (p*K* = 8.0), and the side reaction may occur under the solvent conditions where the cysteine residue of D234eTm is modified with the fluorescence donor. Furthermore, the extra dipeptide may affect the mode of binding of tropomyosin to actin. Then, we expressed D234bTm without the extra dipeptide at the N-terminus with the Sf9-baculovirus system, of which the N-terminus is acetylated as in the case of skeletal muscle Tm. In the case of AEDANS-D234bTm, Förster's critical distance, R_0, was calculated to be 43.3 Å for FLC-F-actin and 37.3 Å for DABMI-F-actin.

The fluorescence spectra of AEDANS bound to D234bTm on the reconstituted thin filaments in the presence and absence of an acceptor (FLC bound to actin) were measured in buffer F + 50 μM $CaCl_2$ for the $+Ca^{2+}$ state or +1 mM EGTA for the $-Ca^{2+}$ state at 20°C (Fig. 5). The donor fluorescence was significantly quenched in the presence of the acceptor (FLC-F-actin) to the same extent as that of D234eTm, and removal of free Ca^{2+} ions from Tn did not change the spectra in either the presence or absence of the acceptor as in the case of D234eTm. The extent of quenching in the case of AEDANS-D234bTm was exactly the same as in that of AEDANS-D234eTm. Therefore, the side reaction did not occur and the extra dipeptide at the N-terminus did not affect the mode of binding of Tm to actin.

To obtain more quantitative data for the transfer efficiency, the ratio of the donor fluorescence quenching was measured by titrating AEDANS-Tm/Tn or AEDANS-D234bTm/Tn with FLC-F-actin (Fig. 6). The fluorescence of AEDANS-D234bTm decreased gradually in the actin/Tm molar ratio range up to 4 and was saturated over 4, instead of 7 in the case of AEDANS-Tm. The extent of the decrease in the relative fluorescence intensity did not change, regardless of whether Ca^{2+} was present or not in either the case of AEDANS-D234bTm or AEDANS-Tm. From the saturation points, the apparent energy transfer efficiencies were calculated to be 0.23 ± 0.03 for AEDANS-Tm and 0.49 ± 0.03 for AEDANS-D234bTm, which corresponds to distances of 52.6 ± 1.6 Å for AEDANS-Tm and 43.6 ± 0.9 Å for D234bTm.

Using DABMI-F-actin as the acceptor, the same titration experiments were carried out, and the distances from Cys-374 of actin were determined to be 42.1 ± 0.7 Å for AEDANS-Tm and 40.5 ± 0.9 Å for AEDANS-D234bTm. These transfer efficiencies and distances are summarized in Table II.

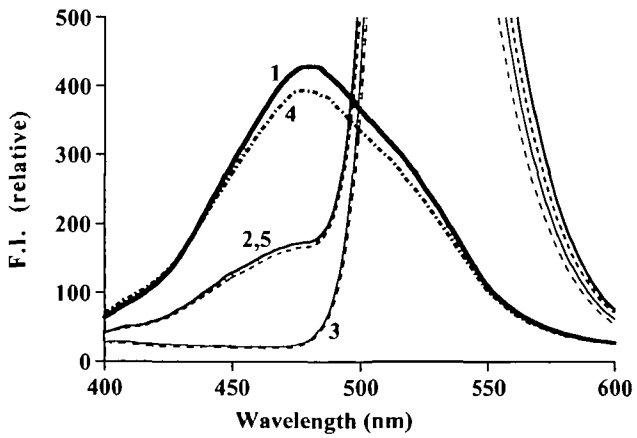

Fig. 5. **Fluorescence spectra of AEDANS bound to Cys-190 of D234bTm on reconstituted thin filaments in the presence and absence of an acceptor (FLC bound to Gln-41 of actin).** (1) F-actin/AEDANS-D234bTm/Tn/+Ca, (2) FLC-F-actin/AEDANS-D234bTm/Tn/+Ca, (3) FLC-F-actin/D234bTm/Tn/±Ca, (4) F-actin/AEDANS-D234bTm/Tn/–Ca, (5) FLC-F-actin/AEDANS-D234bTm/Tn/–Ca. Spectra were measured at 20°C in buffer F and 50 μM $CaCl_2$ for the $+Ca^{2+}$ state (solid lines) or 1 mM EGTA for the $-Ca^{2+}$ state (broken lines). The concentrations of actin, D234bTm, and Tn were 0.2, 0.044, and 0.046 mg/ml, respectively. Excitation was at 340 nm.

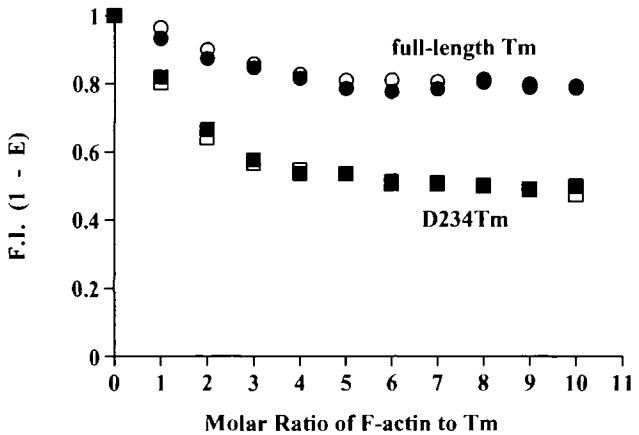

Fig. 6. **Relative fluorescence intensities of AEDANS bound to Cys-190 of Tm (● for $+Ca^{2+}$ and ○ for $-Ca^{2+}$ state) or D234bTm (■ for $+Ca^{2+}$ and □ for $-Ca^{2+}$ state) on reconstituted thin filaments *vs.* molar ratios of FLC-F-actin to Tm.** Values were obtained in buffer F and 50 μM $CaCl_2$ for the $+Ca^{2+}$ state or 1 mM EGTA for the $-Ca^{2+}$ state at 20°C, after correction of the inner filter effects according to Eq. 5. The concentrations of Tm and Tn were 0.044 and 0.046 mg/ml, respectively. Excitation was at 340 nm and emission was measured at 460 nm.

Effects of S1 Binding on FRET between AEDANS-Tn and FLC- or DABMI-Actin on Wild-Type and Mutant Thin Filaments—Fluorescence spectra of AEDANS bound to Cys-133 of TnI on reconstituted thin filaments were measured in the presence of S1, using FLC or DABMI bound to actin as the fluorescence acceptor (Fig. 7). The solvent conditions were buffer F + 50 μM $CaCl_2$ for the $+Ca^{2+}$ state and buffer F + 1 mM EGTA for the $-Ca^{2+}$ state at 20°C. In the absence of an acceptor, the spectra did not change appreciably on the addition of S1 (1/3 mole ratio to actin). But in the presence of an acceptor, the addition of S1 increased the donor fluorescence intensity significantly for both the $+Ca^{2+}$ and $-Ca^{2+}$ states, regardless of whether wild-type or mutant thin filaments were involved. The addition of ATP (1 mM) completely reversed the changes in FRET induced by rigor S1 binding, and after the consumption of ATP through hydrolysis the changes in FRET were again observed. When NEM-treated S1 (1/3 mole ratio to actin) was used instead of normal S1, these increases in donor fluorescence intensity on the addition of S1 were observed even in the presence of 1 mM ATP. The results indicate that in addition to a Ca^{2+}-induced conformational change, an S1-induced conformational change occurs in the thin filaments for both the $+Ca^{2+}$ and $-Ca^{2+}$ states regardless of whether the thin filaments are reconstituted with Tm or D234Tm.

TABLE II. **Distances between probes attached to Tm and actin in reconstituted thin filaments in the presence and absence of Ca^{2+} ions.**

Donor site (Cys190 of Tm)	Acceptor site (actin)	R_0(2/3) (Å)	Efficiency (±Ca)	R(2/3) (Å) (±Ca)
Tm	Gln-41	43.0	0.23 ± 0.03	52.6 ± 1.6
	Cys-374	37.1	0.32 ± 0.02	42.1 ± 0.7
D234eTm	Gln-41	42.8	0.40 ± 0.02	45.8 ± 0.6
	Cys-374	36.8	0.38 ± 0.03	39.9 ± 0.9
D234bTm	Gln-41	43.3	0.49 ± 0.03	43.6 ± 0.9
	Cys-374	37.3	0.38 ± 0.03	40.5 ± 0.9

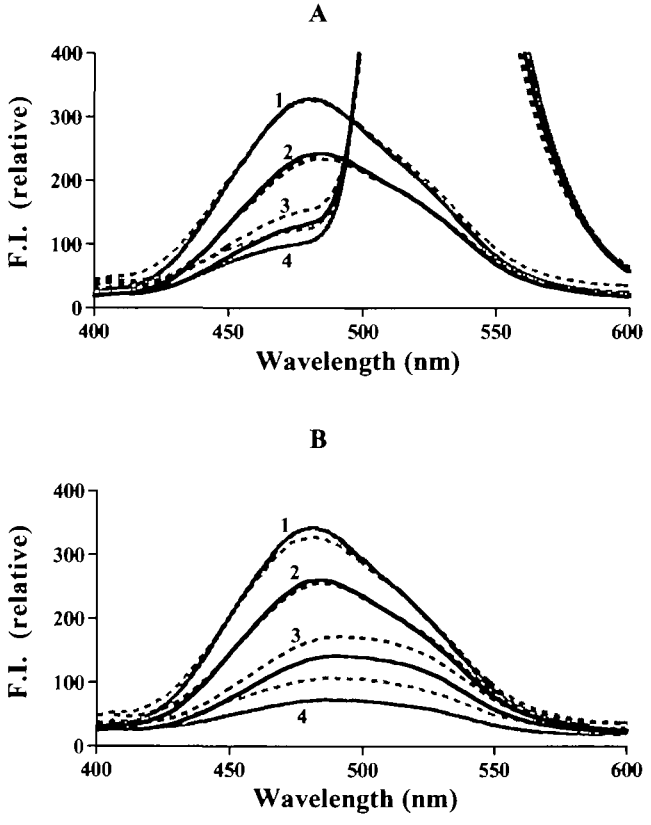

Fig. 7. **Fluorescence spectra of AEDANS bound to Cys-133 of TnI on reconstituted wild-type thin filaments in the presence (broken lines) and absence (solid lines) of S1.** The resonance energy acceptor (Ac) was FLC (A) or DABMI (B), attached to Gln-41 or Cys-374 of actin, respectively. (1) F-actin/ Tm/AEDANS-Tn/–Ca, (2) F-actin/Tm/AEDANS-Tn/+Ca, (3) Ac-F-actin/Tm/AEDANS-Tn/+Ca, (4) Ac-F-actin/Tm/AEDANS-Tn/–Ca. Spectra were measured at 20°C in buffer F and 50 μM $CaCl_2$ for the $+Ca^{2+}$ state or 1 mM EGTA for the $-Ca^{2+}$ state. The concentrations of actin, Tm, Tn, and S1 were 0.2, 0.044, 0.046, and 0.2 mg/ml, respectively. Excitation was at 340 nm.

NEM-treated S1 binds tightly to actin, even in the presence of ATP, and it activates thin filaments that are inhibited by Ca^{2+}-free wild-type Tn-Tm (*39, 40*). It has also been reported that the Ca^{2+}-independent inhibition by D234Tm was largely reversed by NEM-treated S1 (*24*). These results show that the S1-induced conformational change observed with FRET measurements is well correlated to the active state (open state) of thin filaments.

To obtain more quantitative data for the S1-induced con-

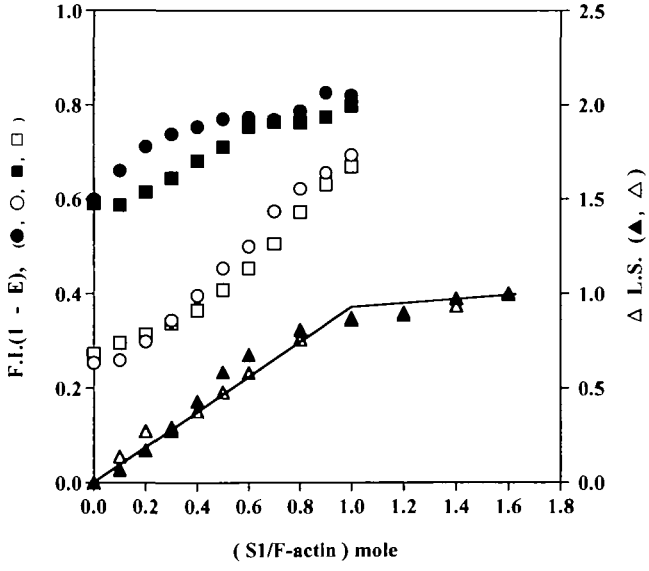

Fig. 8. **Relative fluorescence intensities (1–E) of AEDANS bound to Cys-133 of TnI in reconstituted thin filaments with Tm (● for $+Ca^{2+}$ and ○ for $-Ca^{2+}$ state) or D234eTm (■ for $+Ca^{2+}$ and □ for $-Ca^{2+}$ state) *vs.* molar ratio of S1 to actin.** Values were obtained in buffer F and 50 μM $CaCl_2$ for the $+Ca^{2+}$ state or 1 mM EGTA for the $-Ca^{2+}$ state at 20°C. A small volume of a concentrated S1 solution was added stepwise. For correction of dilution effects and S1-binding effects, a sample containing non-acceptor-labeled F-actin instead of DABMI- F-actin was used as the reference, and the ratio of fluorescence intensities was determined. The concentrations of F-actin, Tm, and Tn were 0.23, 0.044, and 0.046 mg/ml, respectively. Fluorescence measurements were carried out after hydrolysis of contaminating ATP (less than 10 μM). Excitation was at 340 nm and emission was measured at 490 nm. The binding of S1 and thin filaments was monitored as the light scattering intensity (LS) at 550 nm under the same solvent conditions as for fluorescence measurements for wild-type thin filaments in the presence of Ca^{2+} (▲), and mutant thin filaments in the absence of Ca^{2+} (△). Instead of DABMI-F-actin, non-labeled F-actin was used for scattering measurements.

formational change, changes in the FRET efficiency of AEDANS-Tm or -D234Tm/Tn/DABMI-F-actin were measured by the addition of various amounts of S1 in the presence and absence of Ca^{2+} (Fig. 8). Before the addition of S1, the relative fluorescence intensities (1-E) showed a large difference between in the absence and presence of Ca^{2+}, but no difference between wild-type and mutant thin filaments. The extent of the S1-induced conformational change increased as the molar ratio of S1 to actin increased, and was saturated at a molar ratio of ~1 in the presence of Ca^{2+} on both wild-type and mutant thin filaments. Assuming that all thin filaments are in the S1-induced state at the molar ratio of 1, the distance between Cys-133 of TnI and Cys-374 of actin on wild-type and mutant thin filaments was 47.0 ± 0.5 Å in the S1-induced state. The extent of the S1-induced conformational change increased as the molar ratio of S1 to actin increased even in the absence of Ca^{2+}. The relative fluorescence intensities (1-E) on wild-type and mutant thin filaments at the molar ratio of 1 were close to those in the presence of Ca^{2+}.

It should be emphasized here that curves of the relative fluorescence intensity *vs.* molar ratio of S1 to actin in Fig. 8 had different shapes. The curve for wild-type thin filaments in the presence of Ca^{2+} is hyperbolic, whereas that for mutant thin filaments is sigmoidal. In the absence of Ca^{2+}, the curves are sigmoidal for both wild-type and mutant thin filaments. On the other hand, the light scattering intensity increased linearly with increasing molar ratio of S1 to actin up to 1 on both wild-type and mutant thin filaments regardless of whether Ca^{2+} was present or not (Fig. 8).

FRET between AEDANS-Tm and FLC- or DABMI-Actin on Wild-Type and Mutant Thin Filaments in the Presence of S1—In order to detect S1-induced movement of Tm, as predicted by the steric blocking theory, the effect of S1 binding on FRET between probes attached to Cys-190 of Tm or D234Tm and Gln-41 or Cys-374 of actin was measured. Fluorescence spectra of AEDANS bound to Cys-190 of Tm and D234Tm on reconstituted thin filaments in the presence of S1 were measured, using FLC or DABMI bound to actin as the fluorescence acceptor. The solvent conditions were buffer F + 50 μM $CaCl_2$ for the $+Ca^{2+}$ state and buffer F + 1 mM EGTA for the $-Ca^{2+}$ state at 20°C. The spectra of donor fluorescence did not change appreciably on the addition of S1 (1/3 mole ratio to actin) for both the $+Ca^{2+}$ and $-Ca^{2+}$ states, regardless of whether wild-type or mutant thin filaments were involved. The same measurements were carried out in the presence of ATP. The addition of S1 did not change the donor fluorescence intensity, as in the absence of ATP. Furthermore, the effect of NEM-treated S1 (1/3 mole ratio to actin) on the transfer efficiency was measured under the same experimental conditions as for native S1, but no appreciable change in the transfer efficiency due to S1-induced Tm movement was detected.

DISCUSSION

D234Tm—In the present study, deletion mutant D234Tm was used for FRET measurements in order to understand the interaction between Tm or Tn and actin in a reconstituted thin filament, since it lacks the function of Ca^{2+}-induced activation of actoS1 MgATPase activity. Tm expressed by *E. coli* is not acetylated at its N-terminus and consequently the affinity to actin is very low. Several N-terminal extensions, ranging from 2 to 69 amino acids, to mimic the acetylation present in native skeletal Tm have been investigated for restoring the actin binding. Functional characterization of these mutants, such as head to tail polymerization and regulation of the actomyosin ATPase, have shown that many mutants are clearly not native-like in terms of these properties (*41*). *E. coli*–expressed Tm with the Ala-Ser dipeptide extension is most native like (*38*). Therefore, in D234eTm from *E. coli*, an N-terminal construct was made with an Ala-Ser dipeptide extension to restore the actin binding and the molecular head-to-tail binding (*21*). However, the non-acetylated N-terminal amino acid might be labeled with IAEDANS under the conditions where Cys-190 of the D234Tm from *E. coli* is modified with fluorescence donor IAEDANS. On the other hand, the N-terminus of D234bTm expressed by the Sf9-baculovirus system is acetylated like the native Tm, and therefore the extra dipeptide for restoring the actin binding ability is not necessary.

In the present study, two types of D234Tm expressed by *E. coli* and the Sf9-baculovirus system were used for FRET measurements. For measurement of the distance from actin, there was no appreciable difference between D234Tm expressed by the Sf9-baculovirus system and that expressed by *E. coli.* This suggests that D234eTm is labeled specifically at Cys-190 with IAEDANS and binds to actin in the same way as D234bTm. On the other hand, the distances between probes attached to Cys-190 of D234Tm and Gln-41 or Cys-374 of actin are slightly different from those of full-length Tm. But this does not necessarily mean that the position of D234Tm on an F-actin filament is azimuthally different with that of full-length Tm. Tn is located at its binding site on the Tm molecule on thin filaments. The distances between probes on TnI and actin on a mutant thin filament were almost the same as those on a wild-type thin filament. This suggests that the Tn binding site of D234Tm is located at the same position on an F-actin filament as that of full-length Tm. Therefore, the position of Cys-190 of D234Tm on an F-actin filament is more likely different longitudinally from that of Tm, since D234Tm is shorter than Tm.

Tm Movement—Instead of a two-state model based on Ca^{2+}-induced on-off switching, a three-state model has been proposed in which a thin filament exists in rapid equilibrium between three states, blocked, closed and open, and the equilibrium between the blocked and closed states is calcium-sensitive (*5–7*). In this model, a Ca^{2+}-induced conformational change of troponin-tropomyosin is not sufficient to activate the thin filament, a further conformational change induced by myosin binding to actin being necessary. The states have been described in terms of the position of Tm on the actin filament (*5–9*). In the open state, Tm is located on the inner domain of the actin helix. In the blocked state, Tm moves azimuthally toward the outer domain to block the myosin-binding site on actin. The closed state is kinetically and structurally intermediate, where myosin can bind weakly to actin and Tm partially occludes the myosin-binding site on actin. Based on 3D-EM, Rosol *et al.* (*24*) reported that the Ca^{2+}-induced conformational change of mutant thin filaments containing D234Tm was indistinguishable from that of wild type thin filaments. From the results of kinetic analysis of the effects of D234Tm on thin filament activation, they concluded that a mutant thin fila-

ment is trapped in a Ca^{2+}-induced state and fails to undergo the S1-induced conformational change (*24*). They also showed that inhibition by D234Tm was largely reversed by NEM-S1. However, they did not use NEM S1-treated filaments for 3D-EM, since unbound and aggregated material present in such preparations obscured the thin filament fine structure. They did not detect a specific structural change of a thin filament with D234Tm responsible for the S1-induced conformational change.

The interpretation of both X-ray and 3D-EM measurements has been questioned because they do not take into consideration the presence of Tn and possible changes in its structure with Ca^{2+}, although the mass of Tn is rather larger than Tm. In addition, for these measurements changes within actin accompanying Ca^{2+} or cross-bridge binding to thin filaments are not considered (*10*). Since on electron microscopy the sample is observed after fixing, hydrating and staining, the molecular arrangement of a filament on 3D-EM may be distorted. The resolution of 3D-EM is about 30 Å and the diameter of Tm is about 20 Å. Therefore, it is difficult to assign the conformational change of thin filaments precisely on 3D-EM. On the other hand, the resolution of FRET is extremely high when the transfer efficiency is close to 50%, since the transfer efficiency is a function of the inverse of the sixth power of the distance between probes. A distance change of 1–2 Å can be easily detected with this method. FRET can be useful in solutions where proteins are dynamically interacting with others. Moreover, FRET information can be unambiguously assigned to the labeled protein, although the information is limited to the points of probes.

In contrast to 3D-EM analysis, FRET between probes on Tm or D234Tm (*E. coli* or Sf9-baculovirus system) and actin was not sensitive to the Ca^{2+} ion concentration, which suggests that Ca^{2+}-induced movement of D234Tm does not occur. Furthermore, FRET was not sensitive to S1 binding. Using smooth muscle Tm, Garceffa (*42*) showed 2–6 Å movement of Tm on thin filaments due to myosin heads in the absence of Tn. However, appreciable movement of Tm was not detected in the presence of Tn for both Ca^{2+}-induced and S1-induced conformational changes, in agreement with the present FRET measurements. Graceffa suggested that a considerable azimuthal movement on actin is invisible with FRET since the distance between the donor on Cys-190 of Tm and the acceptor on Cys-374 of actin remains practically constant according to the calculation of Tao *et al.* (*18*). In their calculation, the shape of actin was assumed to be spherical. However, actin consists of two domains and its shape is far from spherical (*43, 44*). Furthermore, not only Cys-374, but several other sites (Gln-41, Lys-61, and the nucleotide binding site) were used for FRET between probes on actin and Tm, but in all cases, FRET was not sensitive to a Ca^{2+}-induced change of thin filaments (*14, 17–19*). Therefore, invisible cases of FRET are negligible. The present study also showed that FRET was not sensitive to Ca^{2+}-induced and S1-induced conformational changes of thin filaments for both D234Tm and Tm.

Tm was labeled at positions 87 and 190, which are located at one-third and two-thirds along whole length of Tm, with fluorescence donor IAEDANS. The distances between these sites on Tm and sites on F-actin did not change on Ca^{2+} binding to Tn (*19*). These results suggest that tropomyosin does not move as a whole molecule, but there is still a possibility that a portion of Tm may move. Based on 3D-EM, Narita *et al.* (*45*) proposed a model in which only the C-terminal part of Tm moves greatly in Ca^{2+}-induced Tm movement, the rest including positions 87 and 190 not moving in agreement with FRET measurements. However, the present FRET measurements showed no movement of D234Tm. If a Ca^{2+}-induced conformational change of a thin filament containing D234Tm can be attributed to Tm movement, D234Tm must be extremely flexible so that a part of a region including Cys-190 stays at the constant position and the rest moves greatly like full-length wild-type Tm. This model seems unlikely.

Tn Movement—In contrast to Tm movement, FRET measurements demonstrated that TnI moves greatly on thin filaments in response to a change in the Ca^{2+} ion concentration (*13–16*). On stopped-flow fluorometry, the time rate of this movement was fast enough to allow this TnI movement on actin filaments to be directly involved in the activation of muscle contraction (*13*). FRET between probes attached at position 9 or 133 of TnI, and at Gln-41, Lys-61, Cys-374 or the nucleotide binding site of actin indicated that the C-terminal and inhibitory domains of TnI move towards the outer domain of actin during inhibition (*16*). Thus, a model was proposed in which Tn cross-links the outer domain of one actin monomer with tropomyosin, which covers seven actin-inner domains along the long-pitch helix (*19*). Although the contribution of Tn movement on 3D-EM analysis had been neglected for a long time, recent 3D-EM demonstrated that the main body of Tn moves towards the outer domain of actin (*45, 46*).

Ca^{2+}-induced movement of TnI was also measured on thin filaments reconstituted with D234Tm as FRET. The transfer efficiency was the same as that of native Tm and strongly dependent on the Ca^{2+} ion concentration, suggesting that Tn on D234eTm functions in the same way as on native Tm. On the other hand, Ca^{2+} binding to Tn did not reverse the inhibitory state of the mutant thin filament to the active state (*21*). Therefore, the Ca^{2+}-induced movement of TnI seems not to be sufficient for activating the thin filament.

S1-Induced State—Our results showed that the binding of S1 under rigor conditions (strong binding of S1) reduced the transfer efficiency between probes attached to TnI and actin on both wild-type and mutant thin filaments, whether Ca^{2+} was present or not. The change in transfer efficiency from the Ca^{2+}-induced to the S1-induced state corresponds to an increase of ~7 Å in distance. With FRET between Cys-117 of TnI and Cys-374 of actin on wild-type thin filaments, the same distance change on S1 binding has been reported recently (*47*). This indicates either that TnI detached further away from actin, or that the outer domain of actin became further away from TnI since Gln-41 and Cys-374 are located on the outer domain of actin. If the latter is the case, the distance between probes on Tm and actin should also be changed by S1 binding, since Tm is located on the inner domain of actin. But the distance between probes on Tm and actin did not appreciably change on S1 binding. Therefore, it seems more likely that TnI detaches further away from actin on S1 binding. Zhou *et al.* (*48*) reported that the binding of S1 to actin-Tm at low levels of saturation caused TnI and TnIC to dissociate from actin-Tm, indicating that TnI and TnIC ($-Ca^{2+}$) bind to the closed

state of actin-Tm and that their binding is greatly weakened in the S1-induced open state. FRET measurements showed that the strong S1-binding induced a further conformational change on both wild-type and mutant thin filaments, whether Ca^{2+} was present or not. This conformational change may correspond to a transition to the open state. It has been reported that in wild-type filaments and mutant filaments containing D234Tm, the thin filament-activated Mg-ATPase rate of unmodified S1 increased on the addition of NEM-S1 (*22*). NEM-S1 binds tightly to actin even in the presence of ATP, and it activates thin filaments that are inhibited by Ca^{2+}-free wild-type Tn-Tm (*39, 40*). The addition of NEM-treated S1 to a D234Tm-reconstituted thin filament decreased the transfer efficiency between TnI and actin to the level of that in the case of the rigor complex even in the presence of ATP, indicating that the strong binding of NEM-treated S1 to actin induced the open state in the D234Tm-reconstituted thin filament. However, in the case of unmodified S1, the addition of ATP completely reversed the changes in FRET induced by the strongly bound S1 on both wild-type and mutant thin filaments, whether Ca^{2+} was present or not. On the other hand, the acto-S1 ATPase-activity is only high in wild-type thin filaments and in the presence of Ca^{2+} under physiological conditions. How can we explain this?

Plots of the extent of the S1-induced conformational change *vs.* added S1 (Fig. 8) showed that the curve for wild-type thin filaments in the presence of Ca^{2+} is hyperbolic (Hill coefficient n = 1.0), whereas that of mutant thin filament is sigmoidal (n = 2.3). In the absence of Ca^{2+}, the curves are both sigmoidal (n = 3.3) on wild-type and mutant thin filaments. The sigmoidal curve indicates that cooperative binding of several S1 molecules on a unit length of actin filament is required to induce the TnI movement. On the other hand, the hyperbolic curve indicates that a single S1 molecule binding on a unit length of actin filament induces the TnI movement. During the acto-S1 ATPase cycle, the fraction of S1 bound to actin is very low, and thus the probability of several S1 molecules stay simultaneously on a unit length of actin filament is extremely low. Therefore, on wild-type thin filaments, the transition to the open state with a low population of rigor S1 is depressed in the absence of Ca^{2+} but not in the presence of Ca^{2+}. On mutant thin filaments, the transition to the open state with a low population of rigor S1 is depressed whether Ca^{2+} is present or not. In other words, there is an allosteric equilibrium between the closed and open states, with the former being major in number. S1·ADP·P_i binds most readily to wild-type thin filaments in the open state and shifts the equilibrium towards the open state. But the binding affinity of S1·ADP·P_i to mutant thin filaments in the open state is not so high as that in the closed state. Then the shift of equilibrium towards the open state is depressed. This explains why D234Tm inhibits the acto-S1 ATPase activity even in the presence of Ca^{2+}. It also explains why wild-type thin filaments activate S1-ATPase under physiological conditions only in the presence of Ca^{2+}, and also why a large excess of S1 releases the inhibition even in the absence of Ca^{2+} (*49*). The present FRET measurements showed distinctive distance changes between TnI and actin corresponding well to the three states of thin filaments, which clearly reflect functional states of thin filaments. However, at present, it is not clear whether the S1-induced Tn movement is the cause or the result of the transition of thin filaments to the open state.

Regulation Model—Tm movement is the critical event for the steric blocking theory. Using the theory as a working hypothesis, many structural works have been performed. However, the steric blocking theory is not the unique solution for the mechanism of regulation of contraction of striated muscle. It is well known that F-actin activates the myosin MgATPase activity strongly but G-actin only weakly. A large conformational difference between G-actin and F-actin monomers is not detected. A proper arrangement of myosin binding sites along an actin filament is critical for an active interaction between actin and myosin. Thus, a small conformational change in the F-actin monomer may be sufficient for on-off transition instead of Ca^{2+}-induced Tm blocking. Although the steric blocking theory is widely accepted, it is possible to explain the regulation mechanism without supposing Tm movement. Thus, we proposed a regulation model (*19, 50*), in which troponin cross-links the outer domain of one actin monomer with tropomyosin, which covers seven actin-inner domains along the long-pitch helix. When the two neighboring TnIs along the long-pitch helix cross-link two actin monomers, they may cause considerable distortion of the actin helix and/or significant inhibition of internal motion of the outer domains of seven actin monomers, which are located between

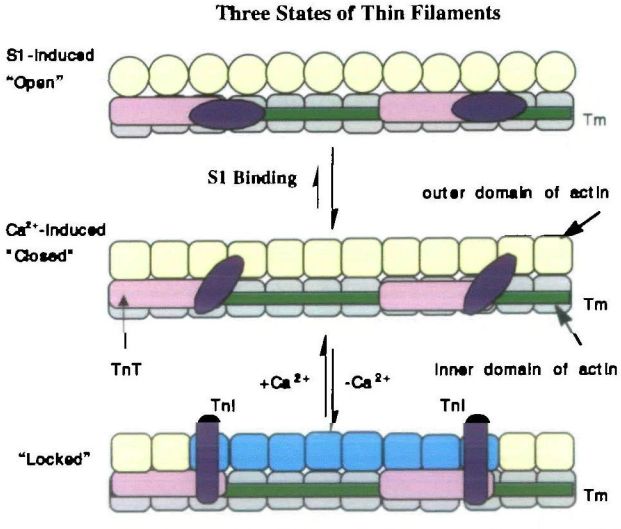

Fig. 9. **A schematic model of Tn and Tm along the long-pitch helix of an actin filament in three states of thin filaments.** One actin molecule is illustrated with two frames that represent its outer and inner domains. One Tm covers the inner domains of 7 actin monomers along the long-pitch helix. In the absence of Ca^{2+}, thin filaments are in the locked state. Two neighboring TnIs along Tm cross-link the outer domains of two actin monomers and lock eight actin monomers in the off-state in combination with Tm. Upon Ca^{2+} binding to TnC, the latchkey of TnI is released, and the thin filament shifts to the closed state (or Ca^{2+}-induced state). In this state, the key is unlocked but the door is still closed. Myosin binding induces a conformational change in actin monomers, and TnI detaches further away from actin. Now the door is open and the thin filament is in the open state. Several strongly bound S1 (rigor complex or NEM-treated S1) molecules on a unit length of an actin filament distort the filament structure, which forces the latchkey of TnI to detach even in the absence of Ca^{2+}. Then, the thin filament is transformed to the open state even in the absence of Ca^{2+}.

two neighboring cross-links along the long-pitch helix. In this model, the inter- and intra-monomer-flexibility of actin on thin filaments play an important role in the regulation. The tropomyosin-troponin complex regulates this flexibility. In fact, there is evidence that Ca^{2+}-binding increases thin filament flexibility (*51–53*).

Flexibility of the hinge region in antibody IgG is essential for its antigen-binding. There are a number of examples indicating that hinge bending domain motion is an essential component for the catalytic activity of enzymes composed of two globular domains separated by a wide cleft (*54–57*). 3D-EM in combination with the atomic structures of actin and S1 revealed that each myosin head interacts with two actin monomers, forming primary and secondary binding sites. The primary binding site on S1 involves interactions with both subdomains 1 and 3 of one actin molecule and a smaller interaction with the next actin molecule down on the actin helix, whereas the secondary site involves a distinct interaction with the neighboring molecule one turn down (*58*). For the smooth moving of a motor, two gear wheels have to fit each other. In analogy to this, the flexibility of actin monomers in thin filaments may play an important role in the fitting precisely of two binding sites of S1 with those of actin on a thin filament. The distortion and/or immobilization of domains of actin monomers in thin filaments by troponin-tropomyosin may disturb a series of actin–myosin interactions (from a weak binding step to a strong binding step) during the ATPase cycle.

In our previous model (*19, 50*), only two states, *i.e.* on- and off-states were considered. However, the present FRET measurements require three states of thin filaments. A new model is illustrated in Fig. 9. Tn acts as a Ca^{2+}-sensing latch. In the absence of Ca^{2+}, Tn in combination with Tm locks the actin monomers in the off-state, and upon binding of Ca^{2+}, this latchkey is released but the door is still closed. In order to open the door completely, S1 binding is required. S1 binding induces the transition to the open state from the closed state, and TnI moves further away from the latching position, or S1 binding induces a further TnI movement and then the transition from the closed state to the open state occurs.

We wish to thank the Food Research and Development Laboratories of Ajinomoto Co. for the generous gift of their microbial transglutaminase, and Prof. I. Muramatsu of Fukui Medical University for kindly providing the rabbit hearts.

REFERENCES

1. Ebashi, S., Endo, M., and Ohtsuki, I. (1969) Control of muscle contraction. *Q. Rev. Biophys.* **2**, 351–384
2. Gordon, A.M., Homsher, E., and Regnier, M. (2000) Regulation of contraction in striated muscle. *Physiol. Rev.* **80**, 853–924
3. Huxley, H.E. (1972) Structural changes in the actin- and myosin-containing filaments during contraction. *Cold Spring Harb. Symp. Quant. Biol.* **37**, 361–376
4. Amos, L.A. (1985) Structure of muscle filaments studied by electron microscopy. *Annu. Rev. Biophys. Biophys. Chem.* **14**, 291–313
5. Mckillop, D.F. and Geeves, M.A. (1993) Regulation of the interaction between actin and myosin subfragment 1: evidence for three states of the thin filament. *Biophys. J.* **65**, 693–701
6. Geeves, M.A. and Lehrer, S.S. (1994) Dynamics of the muscle thin filament regulatory switch: the size of the cooperative unit. *Biophys. J.* **67**, 273–282
7. Lehrer, S.S. and Geeves, M.A. (1998) The muscle thin filament as a classical cooperative/allosteric regulatory system. *J. Mol. Biol.* **277**, 1081–1089
8. Holmes, K.C. (1995) The actomyosin interaction and its control by tropomyosin. *Biophys. J.* **68** (suppl.), 2–7
9. Vibert, P., Craig, R., and Lehman, W. (1997) Steric-model for activation of muscle thin filaments. *J. Mol. Biol.* **266**, 8–14
10. Squire, J.M. and Morris, E.P. (1998) A new look at thin filament regulation in vertebrate skeletal muscle. *FASEB J.* **12**, 761–771
11. dos Remedios, C.G., Miki, M., and Barden, J.A. (1987) Fluorescence resonance energy transfer measurements of distances in actin and myosin. A critical evaluation. *J. Muscle Res. Cell Motil.* **8**, 97–117
12. Miki, M., O'Donoghue, S.I., and dos Remedios, C.G. (1992) Structure of actin observed by fluorescence resonance energy transfer spectroscopy. *J. Muscle Res. Cell Motil.* **13**, 132–145
13. Miki, M. and Iio, T. (1993) Kinetics of structural changes of reconstituted skeletal muscle thin filaments observed by fluorescence resonance energy transfer. *J. Biol. Chem.* **268**, 7101–7106
14. Miki, M. (1990) Resonance energy transfer between points in a reconstituted skeletal muscle thin filament: A conformational change of the thin filament in response to a change in Ca^{2+} concentration. *Eur. J. Biochem.* **187**, 155–162
15. Tao, T., Gong, B.J., and Leavis, P.C. (1990) Calcium-induced movement of troponin-I relative to actin in skeletal muscle thin filaments. *Science* **247**, 1339–1341
16. Miki, M., Kobayashi, T., Kimura, H., Hagiwara, A., Hai, H., and Maéda, Y. (1998) Ca^{2+}-induced distance change between points on actin and troponin in skeletal muscle thin filaments estimated by fluorescence resonance energy transfer spectroscopy. *J. Biochem.* **123**, 324–331
17. Miki, M. and Mihashi, K. (1979) Conformational changes of reconstituted thin filament under the influence of Ca^{2+} ion—Fluorescence energy transfer and anisotropy decay measurements. *Seibutsu-Butsuri* **19**, 135–140 (in Japanese)
18. Tao, T., Lamkin, M., and Lehrer, S.S. (1983) Excitation energy transfer studies of the proximity between tropomyosin and actin in reconstituted skeletal muscle thin filaments. *Biochemistry* **22**, 3059–3066
19. Miki, M., Miura, T., Sano, K., Kimura, H., Kondo, H., Ishida, H., and Maéda, Y. (1998) Fluorescence resonance energy transfer between points on tropomyosin and actin in skeletal muscle thin filaments: Does tropomyosin move? *J. Biochem.* **123**, 1104–1111
20. Hitchcock-DeGregori, S.E. and Varnell, T.A. (1990) Tropomyosin has discrete actin-binding sites with sevenfold and fourteenfold periodicities. *J. Mol. Biol.* **214**, 885–896
21. Landis, C.A., Bobkova, A., Homsher, E., and Tobacman, L.S. (1997) The active state of the thin filament is destabilized by an internal deletion in tropomyosin. *J. Biol. Chem.* **272**, 14051–14056
22. Landis, C., Back, N., Homsher, E., and Tobacman, L.S. (1999) Effects of tropomyosin internal deletions on thin filament function. *J. Biol. Chem.* **274**, 31279–31285
23. Hitchcock-DeGregori, S.E., Song, Y., and Moraczewska, J. (2001) Importance of internal regions and the overall length of tropomyosin for actin binding and regulatory function. *Biochemistry* **40**, 2104–2112
24. Rosol, M., Lehman, W., Craig, R., Landis, C., Butters, C., and Tobacman, L.S. (2000) Three-dimensional reconstruction of thin filaments containing mutant tropomyosin. *Biophys. J.* **78**, 908–917
25. Spudich, J.A. and Watt, S. (1971) The regulation of rabbit skeletal muscle contraction. I. Biochemical studies of the interaction of the tropomyosin-troponin complex with actin and the proteolytic fragments of myosin. *J. Biol. Chem.* **246**, 4866–4871
26. Weeds, A.G. and Pope, B. (1977) Studies on the chymotryptic digestion of myosin. Effects of divalent cations on proteolytic susceptibility. *J. Mol. Biol.* **111**, 129–257
27. Ebashi, S., Wakabayashi, T., and Ebashi, F. (1971) Troponin

and its components. *J. Biochem.* **69**, 441–445
28. Nonaka, M., Sakamoto, H., Toiguchi, S., Kawajiri, H., Soeda, T., and Motoki, M. (1992) Sodium caseinate and skim milk gels formed by incubation with microbial transglutaminase. *J. Food Sci.* **57**, 1214–1241
29. Kim, E., Motoki, M., Seguro, K., Muhlrad, A., and Reisler, E. (1995) Conformational changes in subdomain 2 of G-actin; Fluorescence probing by dansyl ethylenediamine attached to Gln-41. *Biophys. J.* **69**, 2024–2032
30. Kluwe, L., Maeda, K., Miegel, A., Fujita-Becker, S., Maéda, Y., Talbo, G., Houthaeve, T., and Kellner, R. (1995) Rabbit skeletal muscle alpha alpha-tropomyosin expressed in baculovirus-infected insect cells possesses the authentic N-terminus structure and functions. *J. Muscle Res. Cell Motil.* **16**, 103–110
31. Miegel, A., Sano, K., Yamamoto, K., Maeda, K., Maéda, Y., Taniguchi, H., Yao, M., and Wakatsuki, S. (1996) Production and crystallization of lobster muscle tropomyosin expressed in Sf9 cells. *FEBS Lett.* **394**, 201–205
32. Takashi, R. (1988) A novel actin label: a fluorescent probe at glutamine-41 and its consequences. *Biochemistry* **27**, 938–943
33. Lorand, L., Parameswaran, K.N., Velasco, P.T., Hsu, L.K.-H., and Siefring, G.E., Jr. (1983) New colored and fluorescent amine substrates for activated fibrin stabilizing factor (Factor XIIIa) and for transglutaminase. *Anal. Biochem.* **131**, 419–425
34. Lamkin, M., Tao, T., and Lehrer, S.S. (1983) Tropomyosin-troponin and tropomyosin-actin interactions: a fluorescence quenching study. *Biochemistry* **22**, 3053–3058
35. Hudson, E.N., and Weber, G. (1973) Synthesis and characterization of two fluorescent sulfhydryl reagents. *Biochemistry* **12**, 4154–4161
36. Scott, T.G., Spencer, R.D., Leonard, N.G., and Weber, G. (1970) Emission properties of NADH. Studies of fluorescence lifetimes and quantum efficiencies of NADH, AcPyADH, and simplified synthetic models. *J. Am. Chem. Soc.* **92**, 687–695
37. Tausky, H.H. and Shorr, E. (1953) A microcolorimetric method for the determination of inorganic phosphorus. *J. Biol. Chem.* **202**, 675–685
38. Monteiro, P.B., Lataro, C., Ferro, J.A., and Reinach, F.C. (1994) Functional α-tropomyosin produced in *Escherichia coli*. *J. Biol.Chem.* **269**, 10461–10466
39. Pemrick, S. and Weber, A. (1976) Mechanism of inhibition of relaxation by N-ethylmaleimide treatment of myosin. *Biochemistry* **15**, 5193–5198
40. Williams, D.L., Greene, L.E., and Eisenberg, E. (1988) Cooperative turning on of myosin subfragment 1 adenosinetriphosphatase activity by the troponin-tropomyosin-actin complex. *Biochemistry* **27**, 6987–6993
41. Urbancikova, M. and Hitchcock-DeGregori, SE. (1994) Requirement of amino-terminal modification for striated muscle alpha-tropomyosin function. *J. Biol. Chem.* **30**, 24310–24315
42. Graceffa, P. (1999) Movement of smooth muscle tropomyosin by myosin heads. *Biochemistry* **38**, 11984–11992
43. Kabsch, W., Mannherz, H.G., Suck, D., Pai, E.F., and Holmes, K.C. (1990) Atomic structure of the actin: DNase I complex. *Nature* **347**, 37–44
44. Holmes, K.C., Popp, D., Gebhard, W., and Kabsch, W. (1990) Atomic model of the actin filament. *Nature* **347**, 44–49
45. Narita, A., Yasunaga, T., Ishikawa, T., Mayanagi, K., and Wakabayashi, T. (2001) Ca^{2+}-induced switching of troponin and tropomyosin on actin filaments as revealed by electron cryomicroscopy. *J. Mol. Biol.* **308**, 241–261
46. Lehman, W., Rosol, M., Tobacman, L.S., and Craig, R. (2001) Troponin organization on relaxed and activated thin filaments revealed by electron microscopy and three-dimensional reconstruction. *J. Mol. Biol.* **307**, 739–744
47. Kobayashi, T., Kobayashi, M., and Collins, J.H. (2001) Ca^{2+}-dependent, myosin subfragment 1-induced proximity changes between actin and the inhibitory region of troponin I. *Biochim. Biophys. Acta* **1549**, 148–154
48. Zhou, X., Morris, E.P., and Lehrer, S.S. (2000) Binding of troponin I and the troponin I-troponin C complex to actin-tropomyosin. Dissociation by myosin subfragment 1. *Biochemistry* **39**, 1128–1132
49. Lehrer, S.S. and Morris, E.P. (1982) Dual effects of tropomyosin and troponin-tropomyosin on actomyosin subfragment 1 ATPase. *J. Biol. Chem.* **257**, 8073–8080
50. Miki, M. (2001) Structural changes between regulatory proteins and actin: A regulation model by tropomyosin-troponin based on FRET measurements in *Molecular Interactions of Actin*, Vol. 2 (Thomas, D.D. and dos Remedios, C.G., eds.) pp. 191–203, Springer Verlag, Heidelberg
51. Ishiwata, S. and Fujime, S. (1972) Effects of calcium ions on the flexibility of reconstituted thin filament of muscle studied by quasielastic scattering of laser light. *J. Mol. Biol.* **68**, 511–522
52. Yanagida, T., Taniguchi, M., and Oosawa, F. (1974) Conformational changes of F-actin in the thin filaments of muscle induced in vivo and in vitro by calcium ions. *J. Mol. Biol.* **90**, 509–522
53. Isambert, H., Venier, P., Maggs, A.C., Fattoum, A., Kassab, R., Pantaloni, D., and Calier, M.F. (1995) Flexibility of actin filaments derived from thermal fluctuations. Effect of bound nucleotide, phalloidin, and muscle regulatory proteins. *J. Biol. Chem.* **270**, 11437–11444
54. Bennett, W.S. and Huber, R. (1984) Structural and functional aspects of domain motions in proteins. *CRC Crit. Rev. Biochem.* **15**, 291–384
55. Ringe, D. and Petsko, G.A. (1985) Mapping protein dynamics by X-ray diffraction. *Prog. Biophys. Mol. Biol.* **199**, 525–537
56. Holland, D.R., Tronrud, D.E., Pley, H.W., Flaherty, K.M., Stark, W., Jansonius, J.N., McKay, D.B., and Matthew, B.W. (1992) Structural comparison suggests that thermolysin and related neutral proteases undergo hinge-bending motion during catalysis. *Biochemistry* **31**, 11310–11316
57. Sharff, A.J., Rodseth, L.E., Spurlino, J.C., and Quiocho, F.A. (1992) Crystallographic evidence of a large ligand-induced hinge-twist motion between the two domains of the maltodextrin binding protein involved in active transport and chemotaxis. *Biochemistry* **31**, 3499–3506
58. Rayment, I., Holden, H.M., Whittaker, M., Yohn, C.B., Lorenz, M., Holmes, K.C., and Milligan, R.A. (1993) Structure of the actin-myosin complex and Its implications for muscle contraction. *Science* **261**, 58–65
59. White, S.P., Cohen, C., and Phillips Jr, G.N. (1987) Structure of co-crystals of tropomyosin and troponin. *Nature* **325**, 826–828